Human Respiration Detection with Commodity WiFi Devices: Do User Location and Body Orientation Matter?

Hao Wang[1,2], **Daqing Zhang**[1,2], **Junyi Ma**[1,2],
Yasha Wang[1,3], **Yuxiang Wang**[1,2], **Dan Wu**[1,2], **Tao Gu**[4], **Bing Xie**[1,2]
[1]Key Laboratory of High Confidence Software Technologies, Ministry of Education, Beijing, China
[2]School of Electronics Engineering and Computer Science, Peking University, China
[3]National Engineering Research Center of Software Engineering, Peking University, China
[4]School of Science, Royal Melbourne Institute of Technology University, Australia
{haowangsei,dqzsei,majunyi,wangyasha,wyxpku,wudan,xiebing}@pku.edu.cn; tao.gu@rmit.edu.au

ABSTRACT
Recent research has demonstrated the feasibility of detecting human respiration rate non-intrusively leveraging commodity WiFi devices. However, is it always possible to sense human respiration no matter where the subject stays and faces? What affects human respiration sensing and what's the theory behind? In this paper, we first introduce the Fresnel model in free space, then verify the Fresnel model for WiFi radio propagation in indoor environment. Leveraging the Fresnel model and WiFi radio propagation properties derived, we investigate the impact of human respiration on the receiving RF signals and develop the theory to relate one's breathing depth, location and orientation to the detectability of respiration. With the developed theory, not only when and why human respiration is detectable using WiFi devices become clear, it also sheds lights on understanding the physical limit and foundation of WiFi-based sensing systems. Intensive evaluations validate the developed theory and case studies demonstrate how to apply the theory to the respiration monitoring system design.

ACM Classification Keywords
H.5.m. Information Interfaces and Presentation (e.g. HCI): Miscellaneous

Author Keywords
The Fresnel Zone; Channel State Information (CSI); WiFi.

INTRODUCTION

With the rapid development of ubiquitous sensing technologies and fast growth of the world aging population, intelligent environments that can monitor and react to elders' daily activities have received a lot of attention [2][14]. While early work focused mainly on environment monitoring and daily-activity recognition, the past few years have witnessed a surge of interest in health threat monitoring to ensure timely intervention and safety for elders, such as fall detection [12][43][38] and vital sign monitoring [13][3]. Respiratory rate is an important vital sign that can indicate progression of illness and decline in health. Abnormal respiration rate, either too high (tachypnea), too low (bradypnea), or absent (apnea), is a sensitive indicator of physiologic distress that requires immediate clinical intervention. Given that nearly 5% of the total population suffers from respiration illnesses such as Sleep Apnea Syndrome and about 30% of people in their seventies are reported to have a respiration disease in developed countries [25], cost-effective and continuous resipration monitoring is essential.

Two common methods for continuous respiration rate monitoring in clinical setting are impedance pneumography and capnography. However, they are expensive and intrusive, preventing these systems from large scale deployment at ordinary homes with elders. In order to minimize the discomfort brought by the invasive respiration measurement methods, several attempts have been made using wearable [28] and pressure sensors [27] for long-term respiration monitoring. While these two types of contact-based sensing methods are more tolerable for elders, the pressure sensor based systems won't be able to measure respiration rate when the subject leaves the bed, while wearable respiration measurement devices have the issues of acceptance or usability for quite a number of elders [10].

Compared to the contact-based respiration sensing methods, contact-free sensing method is more appealing because it neither confines the subject with cables or beds, nor causes discomfort or skin irritation from contact with electrodes or straps [34]. Therefore, a lot of studies have been devoted to noncontact respiration measurement. For example, Penne et al. used a Time-of-Flight camera and applied advanced image processing algorithms to estimate human respiration rate inside a home [32], unfortunately, such camera-based approaches require the subject to face the camera closely besides having privacy concerns and being affected by the lighting conditions. Kondo et al. deployed a laser sensor to measure the chest wall motion during respiration [18], while Min et al. applied an ultrasonic sensor to achieve the same goal [25]. The most widely studied methods are RF based, ranging from Doppler radar [26], UWB radar [36], FMCW radar [3] to USRP (Universal Software Radio Peripheral) based solutions [33]. The basic idea of all those systems is to measure the displacement in the chest of

Permission to make digital or hard copies of all or part of this work for personal or classroom use is granted without fee provided that copies are not made or distributed for profit or commercial advantage and that copies bear this notice and the full citation on the first page. Copyrights for components of this work owned by others than ACM must be honored. Abstracting with credit is permitted. To copy otherwise, or republish, to post on servers or to redistribute to lists, requires prior specific permission and/or a fee. Request permissions from Permissions@acm.org.
UbiComp '16, September 12-16, 2016, Heidelberg, Germany
©2016 ACM. ISBN 978-1-4503-4461-6/16/09. . . $15.00
DOI: http://dx.doi.org/10.1145/2971648.2971744

human subjects during respiration. While these solutions are quite accurate, their costs are usually prohibitively high which make these solutions impractical in the home setting.

In order to come out with a cost-effective home monitoring system, in recent years researchers began to turn their attention to the commodity WiFi devices already installed in the home for contact-free vital sign measurement. Among those efforts, Abdelnasser et al. used WiFi Received Signal Strength (RSS) signal to extract the respiration rate [1]; while Liu et al. and Wu et al. exploited the fine-grained Channel State Information (CSI) [11] to detect the breathing rate with commodity WiFi devices [22][21][42][23]. Even though these works are still in the exploratory stage, they offer a potentially inexpensive means to extend applications to consumer home-healthcare products. While the RSS-based methods are found to be workable only when the subject stays close to the Line-of-Sight (LOS), the CSI-based methods look more appealing as they can capture the subject's respiration rate from a distance, making it viable for long-term respiration rate monitoring.

Even though the WiFi CSI-based respiration sensing solutions look very promising, we notice that all the previous work, including all the 2.4GHz RF-based respiration sensing research, is based on pure empirical experiments and fails to inform when the minute movement due to human respiration is detectable. Furthermore, there lacks a concrete theory to guide the respiration sensing system design.

In this paper we intend to answer the following questions: (1) can human respiration rate be detected in all the places using a pair of WiFi devices inside a room? Are there any differences for respiration detection if people stay in different places and face differently? (2) If we fix two WiFi devices, what are the best, good, bad places and orientations for respiration detection? If we fix one or two people's location and facing, where should we place the WiFi devices in order to optimally measure the respiration rate? (3) What's the theory behind in order to guide the system design? In a nutshell, we not only intend to provide practical guide for the WiFi-based respiration sensing system design, but also develop a theory to reveal the principles of WiFi RF-based activity sensing in general.

In order to answer the above questions, we first introduce the Fresnel Zone concept and the radio propagation properties in free space, then verify the Fresnel model for WiFi radio propagation in indoor amplitudes when a pair of transceivers are placed apart. By analyzing how a static and moving object affects the receiving RF signal using the Fresnel model and radio propagation properties in indoor environment, we derive the mathematical formula characterizing the amplitude and phase of the receiving radio signal given the radio frequency. By further modeling a human as a varying-size semi-cylinder, we develop the theory to relate one's breathing depth, location and orientation to the detectability of respiration rate. Based on the developed theory, we not only provide the sensing map which informs where are the best, good and bad places/orientations for respiration detection (fixing the location of two WiFi devices), but can provide practical guide about the WiFi transmitter/receiver placement when two people lie on the bed expecting to be monitored simultaneously.

The main contributions of this work can be summarized as follows:

1) As far as we know, this is the first work introducing the Fresnel zone model to indoor environment for respiration rate detection using commodity WiFi devices. This work provides general theoretical foundation for exploring subtle movement detection and possibly the sensing limit of RF-based systems.

2) By analyzing how a moving object affects the receiving RF signal and modeling a human as a varying-size semi-cylinder, we develop the theory to relate one's breathing depth, location and orientation to the detectability of respiration by examining the receiving signal strength in the context of the Fresnel Zone.

3) We evaluated the developed theory with extensive experiments. In particular, we used the theory to guide the design of a respiration rate monitoring system in two typical settings.

RELATED WORK

The research for contact-free sensing of vital signs using wireless technologies started in the late 70's [19]. In the past years, various RF-based approaches ranging from Doppler radar [7], UWB radar [8], FMCW radar [3] to USRP based solutions [9] have been explored to sense the human respiration rate. While these works have shown that the vital signs can be detected accurately, as a drawback, they rely on sophisticated and expensive hardware making them impractical for large scale deployment in ordinary homes. The compelling need for a non-intrusive and cost-effective health monitoring system to improve elders' safety has led researchers to work on respiration rate sensing solutions leveraging the existing WiFi devices at home. The closely related work with this paper can be roughly divided into three categories:

RSS based respiration detection. This line of research was first explored by Patwari and Wilson where a network of Zigbee transceivers and advanced signal processing techniques are utilized for extracting respiration rate from the RSS data stream [29][30]. A more cost-effective solution was developed by O.J. Kaltiokallio et al. [17] where only one pair of Zigbee transceivers are deployed to detect the respiration rate from the RSS stream. With similar ideas, Abdelnasser et al. used two commodity WiFi devices to extract one's respiration rate from RSS [1]. The RSS, however, has found to be insensitive for reliably tracking the minute chest movement due to respiration, as the RSS changes caused by exhale and inhale are so small that they can be easily submerged by environmental noise [23]. Therefore, in actual implementation, the subject is requested to stay either between the line-of-sight of the WiFi devices [1], or very close to the Zigbee transceivers assuming that one's breathing is constant and periodic [29][29][17], rendering it impossible for abnormal breathing detection (e.g., apnea).

CSI based respiration detection. Compared to RSS, Channel State Information (CSI) in WiFi devices is richer and more sensitive for detecting one's respiration. WiSleep [22] was the first work to detect human respiration rate for sleep monitoring based on CSI in commodity WiFi devices. This work was extended in [23] where the sleeping postures and abnormal breathing patterns are considered. Liu et al. [21] further proposed to track the vital signs of both breathing rate and heart

rate during sleep by using off-the-shelf WiFi devices. Wu et al. [42] extended the respiration detection from sleeping to standing posture for stationary human detection. However, behind all the systems and encouraging results, we notice that current WiFi-based respiration detection solutions are mainly based on empirical experiments, they fail to answer when the human respiration rate is detectable. Furthermore, there lacks an underlying theory to guide the system design, researchers have to resort to trial-and-error to make the system work.

The Fresnel zone model. The concept of Fresnel zone originated from the research on the interference and diffraction of light in the early nineteenth century [16]. The first mention of using the Fresnel zone concept at Radio Frequency appeared in a 1936 U.S patent [41][4]. From then on, the Fresnel zone model has found various applications ranging from microwave propagation, wireless station placement to antenna design [15]. The recent work [20] applies the Fresnel-Kirchhoff knife-edge diffraction model to localization in sensor networks. Based on the symmetry properties of the diffraction effect caused by human body when the subject appears in a pair of symmetrical grids, they relate one's location to the Received Signal Strength (RSS) in the sensor network with MICAz nodes, achieving meter-level localization resolution in outdoor environment.

In our work, however, we further consider reflection and frequency diversity of the WiFi RF signal in constructing the Fresnel zone model and reveal the signal change pattern in each subcarrier caused by minute movement of a subject. With this new finding, we are able to capture the subtle body displacement on the receiving RF signal at the granularity of RF wavelength, pushing the sensing resolution to an unprecedented centimeter-level. This opens up new opportunities for high-precision human sensing in indoor environment, such as respiration detection.

UNDERSTANDING WIFI FRESNEL ZONE

In this section, we first introduce the basics of the Fresnel zone model in free space, then we qualitatively analyze how a static and moving object affects the receiving RF signal w.r.t. the Fresnel zone. Based on the ideal Fresnel zone model in free space, we design real experiments to verify the existence of the Fresnel zones for WiFi radio propagation in indoor environment. Finally we quantitatively characterize the receiving signal in the presence of a moving object and derive the properties of RF propagation in the context of WiFi Fresnel zone.

The basics of the Fresnel zone model

In the context of radio propagation, Fresnel zones refer to the concentric ellipses with foci in a pair of transceivers. Assume P_1 and P_2 are two transceivers with certain height (as shown in Fig. 1), for a given radio wavelength λ, the Fresnel zones containing n ellipses can be constructed by ensuring:

$$|P_1Q_n| + |Q_nP_2| - |P_1P_2| = n\lambda/2$$

where Q_n is a point in the nth ellipse. While the innermost ellipse is defined as the 1st Fresnel zone, the elliptical annuli between the first ellipse and the second is defined as the 2nd Fresnel zone, and the nth Fresnel zone corresponds to the

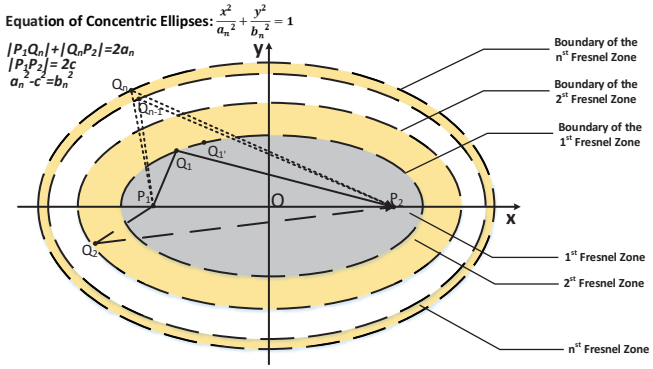

Figure 1. Geometry of the Fresnel zone.

elliptical annuli between the $(n-1)$th and nth ellipses. As the boundary between two adjacent Fresnel zones is an ellipse, we further define the boundary of the nth Fresnel zone as the ellipse between nth and $(n+1)$th Fresnel zones:

$$b_n = \{Q_n, P_1, P_2 \,|\, |P_1Q_n| + |Q_nP_2| - |P_1P_2| = n\lambda/2\} \quad (1)$$

Apparently, the width of the Fresnel zone keeps decreasing as n changes from 1 to N, approaching $\lambda/2$. According to the previous research, the significant zones for RF transmission are the first $8-12$ zones, more than 70% of the energy is transferred via the first Fresnel zone [15].

How a static/moving object affects the receiving RF signal

As shown in Fig. 1, P_1, P_2 are a pair of transceivers in free space. When P_1 sends a radio signal to P_2, the amplitude and phase shift of received signal are determined by the length of P_1P_2 (LOS).

Assume a static object appears at the boundary of the first Fresnel zone, Q_1 in Fig. 1, an additional signal path is introduced from the object and the received signal at P_2 is a linear combination of the reflected signal and signal via LOS. Because the source signal is the same, while the path length of the reflected signal ($P_1Q_1P_2$) is $\lambda/2$ longer than the length of LOS, the phase difference between the two signals is π, adding the phase shift π introduced by the reflection [15], the two signals have the same phase but different amplitude, leading to a superposed stronger received signal.

But if we put the object at the boundary of the second Fresnel zone, as the path length of the reflected signal is λ longer than that of the signal via LOS, the phase difference between the two signals is 2π. Considering the additional phase shift π, the received signals would have destructive phases, causing the two signals canceling each other. Similarly, when the object is located at the boundary of an odd number Fresnel zone, the reflected signal would enhance the receiving signal at P_2 as it is in-phase with the LOS signal; when the object is located at the boundary of an even number Fresnel zone, the reflected signal and LOS signal would cancel each other as they have destructive phases, thus P_2 would observe weaker signal than that without any object in the space.

Now assume an object moves from the 1st Fresnel zone to the nth Fresnel zone, while the signal traveling via LOS remains

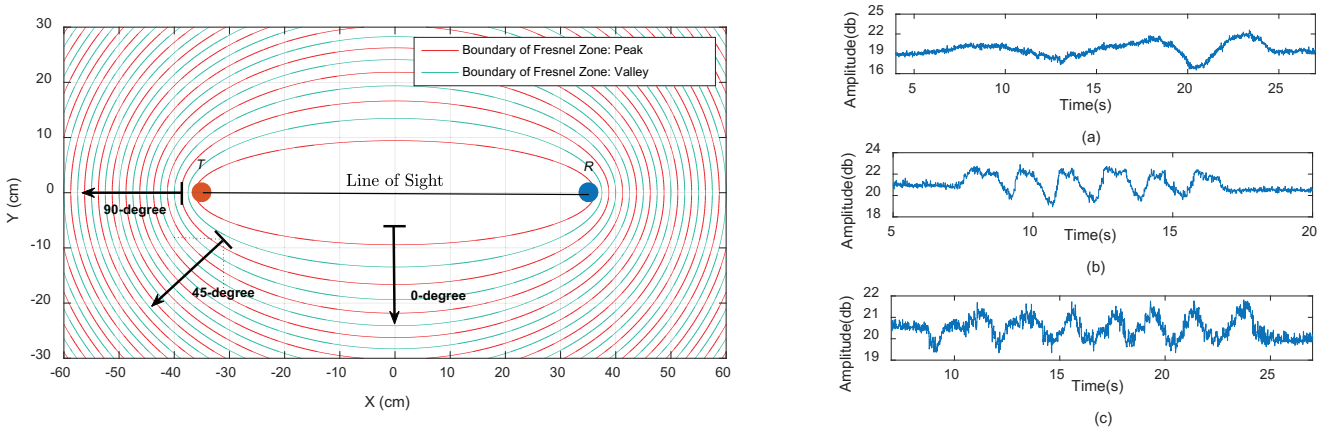

Figure 2. WiFi Fresnel zone experimental settings (left) and results (right): (a) 0-degree, (b) 45-degree, (c) 90-degree.

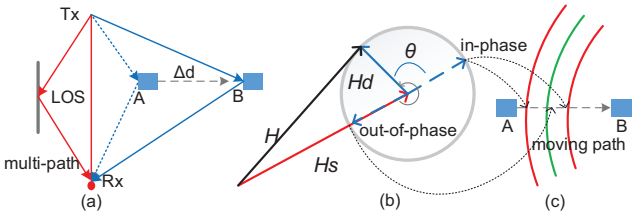

Figure 3. Representation of linear superposition of multi-paths.

the same, the signal reflected by the object changes over time. For the amplitude of the reflected signal received at P_2, as the object moves outward leading to longer traveling distance, thus the amplitude of the signal will decrease gradually. For the phase of the reflected signal received, as the object moves outward across different Fresnel zones, the phase difference between the two signals increase continuously from 2π to 3π, 4π, ..., $(n+1)\pi$, leading to the changing signal superposition. According to basic interference principle, the received signal will present peaks or valleys when the object crosses the boundaries of the Fresnel zones. However, if the object moves along ellipses, as there is no length change for the reflected signal path, the received signal remains the same.

While all the above analyses are based on theory and assumption in free space, does the Fresnel Zone model exist in multipath-rich indoor environment? What happens when an object moves along different directions?

Verifying WiFi Fresnel Zone in indoor environment

In this section, we intend to verify the existence of WiFi Fresnel Zone in indoor environment through experiments.

Experimental settings: We use two WiFi devices placed 70cm apart and a metal cup with a diameter of 7cm and height of 19cm to conduct the experiment in an office room. We leverage the commonly used vertically polarized antennas and place them vertically to the ground with 70cm height. Also the antennas and the metal cup are placed in the same horizontal plane so that the electric field is perpendicular to the plane of incidence. As researchers empirically assume that a free-space radio propagation [5] means no obstruction or reflection in the space bounded by the "first several zones", while the significant zones for RF transmission are the first 8~12 Fresnel zones [15]. Thus in our experiment, we keep the first 12 Fresnel zones clear from obstruction or reflection, and choose one subcarrier for evaluation, e.g., $f = 5.24GHz$.

Experimental Protocol: We first draw the Fresnel concentric ellipses with two foci corresponding to the above setting in Fig.2 (left), the boundaries of Fresnel zones are colored in blue and red. In order to verify the existence of WiFi Fresnel zone, we move the metal cup along the perpendicular bisector (0-degree) from the 1st to the 6th Fresnel zone. What we expect to observe are five valleys and peaks presented alternately, where the first one should be a peak as a result of crossing the boundary of the 1st Fresnel zone. In order to verify that the WiFi Fresnel zones are in shape of concentric ellipses, we move the metal cup along three paths with the same distance of 15cm as shown in Fig.2 (left), labeling as 0-degree,45-degree and 90-degree. The total number of valleys/peaks we observe for these three paths should be 5, 11 and 14, respectively, corresponding to the number of zone boundaries crossed.

Experimental results: (1) The occurrence sequence of valleys and peaks match the Fresnel model, e.g., the first peak shows up correctly when the object reaches the boundary of the 1st Fresnel zone, followed with a valley when the object reaches the second, see Fig.2 (a). (2) The occurrence time and number of valleys/peaks for each path correctly match the Fresnel model, i.e., WiFi Fresnel zone is in the shape of concentric ellipses with foci in points T and R, e.g., the number of valleys and peaks along the perpendicular bisector is 5, see Fig.2 (a) and along the 45-degree path is 11, see Fig.2 (b), which are the number of the Fresnel zone boundaries the object crosses over, respectively. (3) When the object crosses a series of Fresnel zones, the receiving signal shows a continuous sinusoidal-like wave besides the expected peaks and valleys, verifying the expected phase change.

Characterizing the receiving signal in the presence of a moving object

In order to characterize the receiving signal in the presence of a moving object, we study a typical setting as shown in

Fig.3 (a) in which a transmitted signal arrives at the receiver through multiple paths. We divide all these paths into static and dynamic ones, then the receiving signal $H(f,t)$ can be denoted as a phase vector with the following equation [35][39]:

$$H(f,t) = H_s(f) + H_d(f,t) = H_s(f) + a(f,t)e^{-j2\pi d(t)/\lambda}$$

where the static vector $H_s(f)$ is the sum of signals from static paths while the dynamic vector $H_d(f,t)$ is introduced by the reflected signal from the moving object as shown in Fig.3 (b). The reflected signal can be further represented by a vector, where $a(f,t)$ is the complex valued representation of amplitude and initial phase offset of the dynamic path, $e^{-j2\pi d(t)/\lambda}$ is the phase shift on the dynamic path length $d(t)$. Apparently when the length of the reflected signal changes by λ, its phase shifts 2π (rotates one round). Hence the receiving signal $H(f,t)$ has time-varying amplitude in complex plane:

$$|H(f,\theta)|^2 = |H_s(f)|^2 + |H_d(f)|^2 + 2|H_s(f)||H_d(f)|cos\theta \quad (2)$$

where θ is the phase difference between the static vector $|H_s(f)|$ and dynamic vector $|H_d(f)|$. In particular, when the object moves for a short distance, e.g., several wavelengths as in Fig.2 (a), it is safe to assume the amplitude of the dynamic vector remains the same, i.e., $|H_d(f)|$ is const. This explains why the amplitude of the receiving signal looks like a sinusoidal wave when the object crosses several Fresnel zones. Specifically, the peaks appear when $\theta = 2\pi, 4\pi, ...$ and the valleys show when $\theta = 3\pi, 5\pi, ...$, corresponding to the boundaries of the Fresnel zones.

WiFi RF propagation properties in indoor space

With the above discussions, we summarize the WiFi RF propagation properties in indoor space as follows:

1) WiFi Fresnel zones take the shape of concentric ellipses with foci in a pair of transceivers which can be calculated mathematically.

2) A moving object usually produces a reflected signal with varying amplitude and phase. In a small moving scale, the reflected signal roughly has fixed amplitude with varying phase affecting the received signal. In a large moving scale, the reflected signal experiences both phase change and amplitude variation as input to the received signal.

3) When an object crosses a series of Fresnel zones, the receiving signal shows a continuous sinusoidal-like wave, with peaks and valleys generated by crossing the boundaries.

4) If the reflected signal by a moving object changes the path length by λ, its phase will undergo a change of 2π, generating a complete sinusoidal cycle; if the reflected signal changes the path length shorter than λ, the generated signal is a fragment of the sinusoidal cycle.

SENSING HUMAN RESPIRATION IN WIFI FRESNEL ZONE

In this section, we first model a human as a varying-size semi-cylinder simulating the chest movement during respiration, then we convert the chest displacement to phase change to characterize how human respiration affects the resultant receiving signal. By relating this phase change to one's location/orientation, we develop the theory on the detectability of respiration w.r.t. the Fresnel model. Then we show when and how frequency diversity can help respiration detection. Finally, we study a multi-user respiration sensing scenarios.

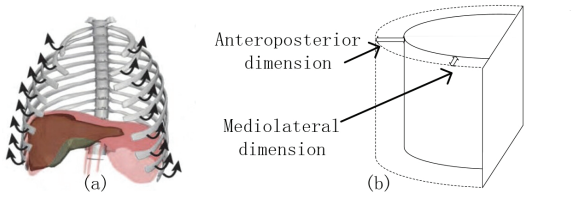

Figure 4. (a) Physiological behavior during respiration, and (b) semi-cylinder respiration model.

Modeling Human Respiration

Human respiration is a process consisting of the cyclical inflation and deflation of the lungs. Motions and deformations that are described from the ribcage are shown in Fig.4 (a) [37]. The chest displacement during respiration is $4.2 \sim 5.4mm$ in anteroposterior dimension, and $0.6 \sim 1.1mm$ in mediolateral dimension [24]; while in the deep inspiratory breath hold (DIBH), this displacement can be increased up to $12.6mm$ in anteroposterior dimension [31]. Hence, we model the person as a varying-size semi-cylinder, as shown in Fig. 4(b), where the outer and inner cylinder surfaces correspond to the chest positions for exhale and inhale, respectively.

Converting chest displacement to phase change

In order to sense the respiration rate of a person, we view the human body as the reflection surface (see Fig.5 (a)) and study how the chest displacement due to respiration affects the received RF signal as a moving object. To this end, we first convert the chest displacement to the change of the reflected path length, and then convert this path length change to phase change. Let Δd be the distance of the chest displacement, then the path length change caused by the chest movement is around (no more than) $2\Delta d$ [39]. If the path length of the reflected signal changes continuously by a wavelength λ, the resultant reflected signal will exhibit a phase change (rotation) of 2π. Thus as shown in Fig.5 (b), the phase rotation θ caused by respiration can be calculated by the following equation:

$$\theta \approx 2\pi * 2\Delta d/\lambda \quad (3)$$

Where λ is around 5.7cm (for 5GHz) and 11cm (for 2.4GHz). As the mean distance of chest movement Δd in anteroposterior for normal respiration and deep respiration like DIBH are around $5mm$ and $12mm$, respectively [24] [31], the resultant phase change θ is between 60°to 150°.

Because the reflected signal experiences a phase change of 60°$\sim$ 150°and corresponds to a fragment of sine wave cycle. Now we ask the following questions: how different fragments affect the received signal? where are the best and worst position of the fragment in the sine wave cycle?

Human location vs resultant receiving signal

According to equation (2), we know that the amplitude of the received signal $H(f,t)$ is related to the $cos\theta$ term when H_s and H_d are constant. It's noted that $H(f,t)$ looks like a sine wave when the moving object crosses several wavelengths,

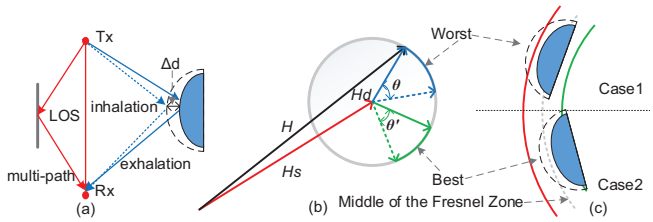

Figure 5. Human Location in the Fresnel Zone.

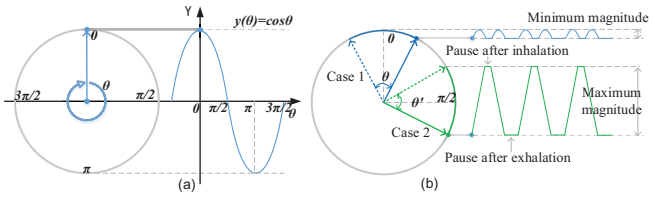

Figure 6. Magnitude and waveform of the resultant receiving signal for different human locations.

corresponding to several cycles and Fresnel zones. But for a normal respiration with phase change between 60°to 150°, the receiving signal $H(f,t)$ is definitely not a sine wave anymore, so how does it look like? As one respiration cycle consists of an inhalation followed by a pause and an exhalation followed by another pause, and human respiration is usually periodical, then according to equation (2), the receiving signal $H(f,t)$ also consists of four parts: a waveform generated by inhalation, a straight line caused by the pause after inhalation, a waveform generated by exhalation, and another straight line caused by the pause after exhalation.

As we already know that the phase change θ caused by inhalation or exhalation is between 60°to 150°and it lies in the cycle of cosine wave (see Fig. 6 (a)), then both the angle of θ and its position affects the shape of the signal waveform of $H(f,t)$. Assume $\theta = \pi/3$ which corresponds to a normal breath, if the angle covers the range from $-\pi/6$ to $\pi/6$ as shown in Fig. 6 (b), then we can see a small arc produced by the term $cos\theta$ during inhalation and another small arc produced by exhalation. In this worst case, not only the magnitude of the waveform is small due to small variation of $cos\theta$ when $\theta = 0$ or π, but one cycle contains more than one peak/valley as well. But if the angle covers the range from $\pi/3$ to $2\pi/3$ as shown in Fig. 6 (b), then we can see a big trapezoid-like waveform produced by the inhalation and exhalation cycle. Assume $\theta = 2\pi/3$ which corresponds to a deep breath, let the angle cover the range from $\pi/6$ to $5\pi/6$, then we have even a bigger trapezoid like waveform produced by the inhalation and exhalation cycle. Apparently, in order to make the respiration rate easy to extract correctly from the receiving signal, it is expected that the θ angle not only covers a large range but also lies fully in the monotonically changing fragment of the cosine wave (around $\pi/2$ or $3\pi/2$). In particular, the best choice for the cosine wave fragment of a fixed θ is centered around $\pi/2$ or $3\pi/2$, corresponds to the middle of each Fresnel zone.

In conclusion, the receiving signal is affected by both the breathing depth and the human location. Within each Fresnel zone, the worst human location for respiration sensing is

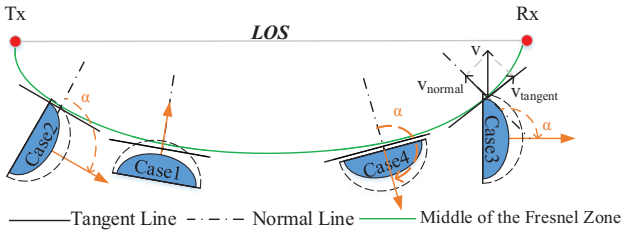

Figure 7. Body Orientation α in the Fresnel zone.

around the boundary, while the best location appears in the middle, as shown in Fig.5 (b)(c). Comparing different Fresnel zones, locating in inner zones incurs stronger reflected signal due to shorter reflection path and makes the receiving signal easier to detect than in outer zones, if the subject appears within the same relative location of Fresnel zones.

Body orientation vs resultant receiving signal

We already know that the chest displacement during respiration is different in anteroposterior and mediolateral dimensions, the body displacement on the back is almost zero during respiration. Hence with the orientation changing, the body displacement for signal reflection changes too. As the variation of the received signal depends on the variation of the reflected signal due to body displacement, it is thus affected by the body orientation besides the breathing depth and body location.

As shown in Fig.7, we assume that the subject is already located at the best location (case 1), e.g, at the middle of the second Fresnel zone. When the subject rotates for 180°, the effective body displacement will change from the biggest to zero, corresponding to the orientation change from facing the LOS to opposing the LOS.

As shown in case 3 of Fig.7, we decompose the body displacement in mediolateral dimension into two components: the effective displacement is along the direction of the normal line, which causes the reflection path length change; the other one along the direction of the tangent line, which causes no change in reflection path. Hence in theory, each orientation has an associated effective body displacement ranging from 0 to $12mm$. For case 1 in Fig.7, as the subject is in parallel with the tangent line facing LOS, the effective body displacement is the largest and it will produce the biggest phase change; For case 2 where the chest of the subject is in parallel with the normal line, as the chest movement in the mediolateral dimension is only around $1mm$ (from $0.6-1.1mm$) [24], the effective body displacement will be small. Further for case 3 and case 4, the effective displacement could be even smaller. In all the cases, whether the generated reflected signal can be detected or not depends not only on the location (affecting the signal magnitude), but also on environment noise.

Fresnel zone vs frequency diversity

So far, we only investigate the Fresnel zone model for a single carrier with frequency f, but actually in WiFi Intel 5300 devices we have the CSI measurement of 30 subcarriers, each subcarrier has its own wave length and frequency. Now let's choose two subcarriers $f = 5.24GHz$, $f' = f + \Delta F$ where

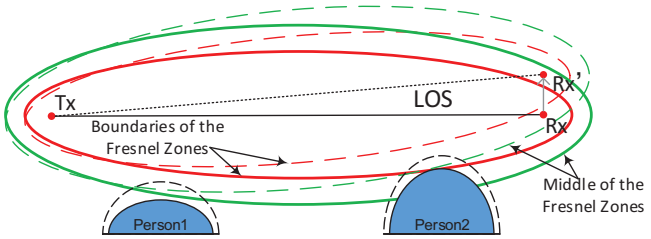

Figure 8. Illustration of two-person respiration detection: the solid green line represents the middle of the Fresnel zone, the red line represents the boundary; the two dash lines correspond to the two lines after moving the device from R_x to R'_x

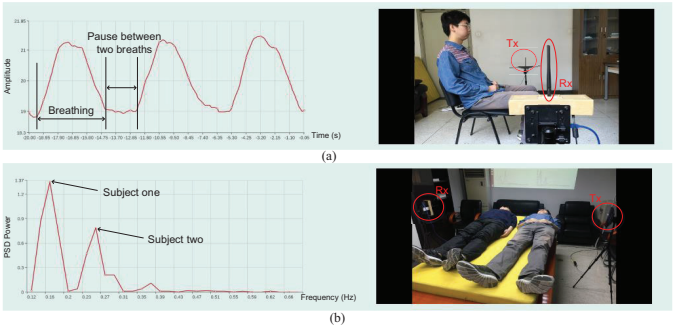

Figure 9. Web-based User Interface.

the frequency interval ΔF between adjacent subcarriers in 802.11n is at most 625KHz for 30 subcarriers and put their Fresnel zones together. Interestingly we notice that for the inner Fresnel zones, these two subcarriers have almost overlapping boundaries; but the difference between their corresponding zone boundaries keeps increasing as the number of zones increases, until the boundary of the ith Fresnel zone of f catches up with $(i+1)$th Fresnel zone of the subcarrier $f^{'}$. From the above observation, we understand that for inner Fresnel zones, if one subcarrier cannot measure the respiration, the other subcarriers cannot either. But starting from certain Fresnel zone outwards, when one's location is close to a bad position (close to the Fresnel zone boundary) for one subcarrier, maybe we can exploit the frequency diversity to find another subcarrier which shows the best or good location for the same position (near the middle of the Fresnel zone).

With this idea in mind, suppose we choose the first subcarrier to sense one's respiration corresponding to a phase angle of $\pi/3$, then we ask the subject locates in the worst place (from $-\pi/6$ to $\pi/6$) for subcarrier 1, from which Fresnel zone m onwards can we always find a subcarrier which has a phase shift of $pai/6$ from subcarrier 1?

To solve this problem, we consider the two extreme subcarriers $f_1 = 5.24GHz$ and $f_2 = f_1 + 29 * \Delta F$ with wavelengths λ_1 and λ_2, respectively. Assume the subject is located at the boundary of the mth Fresnel zone of $f1$. Let c be the speed of light, φ_{ref} be the additional phase shift caused by reflection, L be the LOS length, then the path length P_L of the reflected signal is $P_L = m/2\lambda_1 + L$. The phase difference $\Psi(f)$ between the LOS and the reflected signal is $\Psi(f) = 2\pi f(P_L - L)/c + \varphi_{ref}$, then the phase shift between f_1, f_2 is given by $\Delta\Psi(f_1, f_2) = 2\pi f_2(P_L - L)/c - 2\pi f_1(P_L - L)/c$, bringing f_1, f_2, P_L into the equation:

$$\Delta\Psi(m) = m\pi\Delta F / f_1 \approx 0.0035m\pi \quad (4)$$

Hence m can be derived for $\Delta\Psi(m) >= \pi/6$. The obtained m is 48, which means that if the subject locates outside the 48th Fresnel zone, at least one subcarrier is good for use. For the case that LOS is set to 1m, the 48th Fresnel zone is 108 cm away along the perpendicular bisector of the LOS. Of course, besides frequency diversity, we also need to consider the power loss in the reflected path when the subject is far from transceivers.

Multi-user location vs respiration detectability

Based on the theory developed for a single subject, we now consider sensing two subjects' respiration rates, where the two subjects are assumed to lie on a bed as shown in Fig.8. As the two subjects are viewed as two moving objects in the same static environment, the total receiving signal variance can be approximated as a linear combination of the variance caused by the chest displacement of each person [40]. Assume that the respiration is the only body movement from the two subjects, then the impact of each subject's breathing depth, body location and orientation to the receiving signal is independent and the same as before. Thus, to detect two subjects' respiration rates simultaneously, we need to make sure that the location of each subject is around the middle of an inner Fresnel zone. As an illustration in Fig.8, we show that it is pretty easy to expose two subjects' locations to the middle of a certain Fresnel zone (best place) by fixing their locations while changing the location of one WiFi device. In such a setting, the respiration rate of each person can be extracted in the frequency domain using Power Spectral Density (PSD).

EVALUATION

To validate the theory we developed, we first implement a real-time human respiration detection system using off-the-shelf WiFi devices. We then conduct comprehensive evaluations and report the results in this section.

System Implementation and Experimental Environment

Our prototype system consists of two main modules: *Signal Preprocessing* and *Breathing Rate Estimation*. We follow many design choices as in other systems [6, 21] to understand and validate our theory in real-world contexts.

We collect WiFi CSI, and each CSI stream contains readings from 30 subcarriers. The CSI streams are first handled by *Signal Preprocessing* to reduce noise. In particular, we apply the Hampel filter [6] with a sliding window at each subcarrier to remove outliers which typically have significantly different values from neighboring CSI measurements. In addition, since human respiration rate usually has a low-frequency range, we apply a moving average filter to remove high-frequency noise which is unlikely to be caused by respiration. The resulting CSI streams are then analyzed by *Breathing Rate Estimation* to estimate breathing rate. Specifically, we utilize a threshold based method to select subcarriers having large variance of

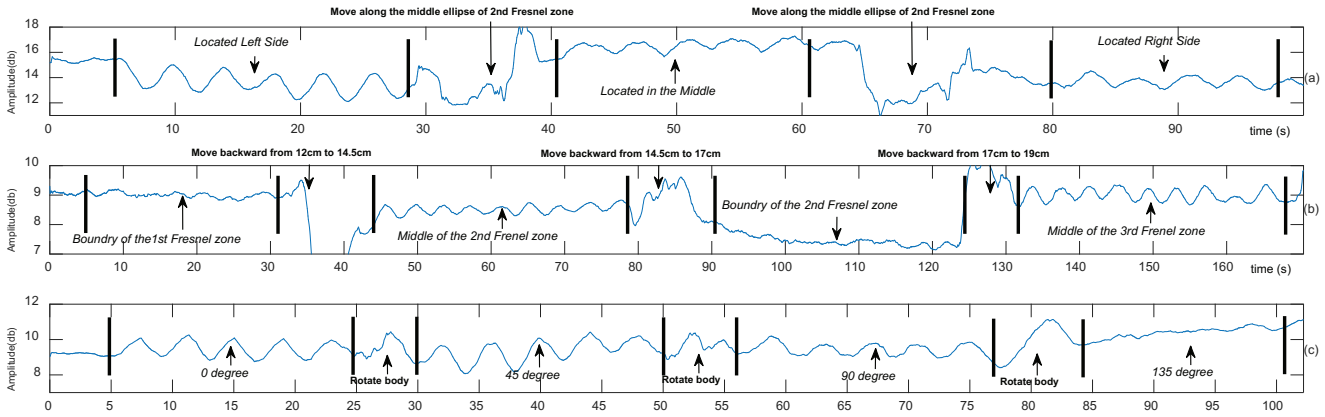

Figure 10. Evaluation of user location and body orientation: (a) moving along the ellipse line with fix body orientation; (b) moving along perpendicular bisector line with fixed body orientation; (c) rotating body orientation with fix user location.

CSI amplitude in a time window as in [21]. For *single-user respiration detection*, to capture the periodic changes caused by chest movements during inhaling and exhaling, we use a Fake Peak Removal algorithm as in [21] to remove peaks which are too close to each other. For *multi-user respiration detection*, since CSI signal is a linear combination of the variance of each subject, we hence use Power Spectral Density (PSD) to transform the time series of CSI measurements on each subcarrier to its power distribution in the frequency domain. A strong periodic signal generates a peak at the frequency corresponding to its period in PSD, e.g., when detecting breathing rate for two subjects, the CSI measurements should present two peaks at the frequency corresponding to that of each subject.

We deploy a prototype system which consists of a WiFi device (i.e., mini-pc) and a commodity wireless access point (i.e., TP-Link WDR5300 with one antenna running on the 5.24GHz channel) in an 802.11n WiFi network. The mini-pc is equipped with an Intel WiFi Link 5300 card for measuring CSI [11] and one external antenna. The packet transmission rate is set to 20pkts/s. We choose and place the antennas same as we did for verifying the Fresnel Zones previously.

Experimental Methodology

We recruit nine participants over a period of three months. Each participant is required to sit on a chair or lie on a bed, breathing normally and naturally. We build a web-based user interface to show the breathing rates along with a real-time video recorded as shown in Fig. 9. When the subject is conducting the experiment, other two subjects are independently watching the video stream to record the ground truth manually.

With the prototype system, we investigate the following two cases: (1) With a pair of WiFi transceivers placed in an indoor environment, can we detect single-user respiration effectively at any location, does user location or body orientation matter, and how do they affect the performance? (2) Given two subjects with fixed user location and body orientation, where do we place WiFi devices to achieve the best performance?

Case 1: Single User with a Pair of WiFi Tx/Rx

We first ask a subject to sit on a chair in an office room. We fix the LOS distance (i.e., 1m apart with 70cm height) between the WiFi Tx and Rx, and evaluate the performance by changing the subject's location and body orientation.

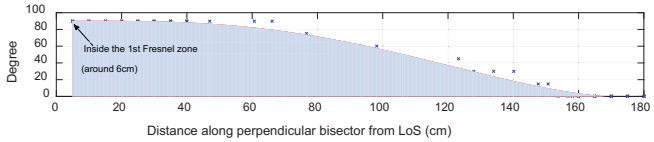

Figure 11. Evaluation of body orientation in different Fresnel zones.

A. Fix LOS Distance

With the LOS distance ($R_1 + R_2$) set to 1m and wavelength (λ) set to 5.7cm (i.e., central frequency 5.24GHz), we first obtain the theoretical ground for Case 1 by computing the Fresnel zone mathematically following Equation (1), e.g., the boundaries of the first three Fresnel zones are 12.05cm, 17.16cm and 21.16cm away from the LOS along the perpendicular bisector, respectively. We then conduct a series of experiments to evaluate the performance by varying user location, body orientation, as well as CSI subcarriers.

(1) Does Subject's Location Matter? In this experiment, with a pair of WiFi Tx/Rx (LOS distance = 1m) placed in an office room, a subject is asked to sit on a chair at different locations, and breath normally with 0° body orientation. We first vary subject's location within the same Fresnel zone. A subject first moves along the middle ellipse of a Fresnel zone (a Fresnel zone can be physically viewed as the area between an inner ellipse and an outer ellipse). Figure 10 (a) shows the results of different locations in the 2nd Fresnel zone. We observe that the CSI signals at different locations along the middle ellipse of the same Fresnel zone are quite consistant and sharp enough to be used for detection. The subject is then asked to move across different Fresnel zones. Figure 10 (b) shows the result when the subject moves along the perpendicular bisector across Fresnel zones 2 and 3. The figure shows that while CSI signals have a strong presence in the middle ellipse of a Fresnel zone, they start fading when moving toward the boundary. We cannot observe clear periodic patterns at each of the boundaries, hence it is likely resulting in detection failure. While we observe a similar phenomenon in each Fresnel zone,

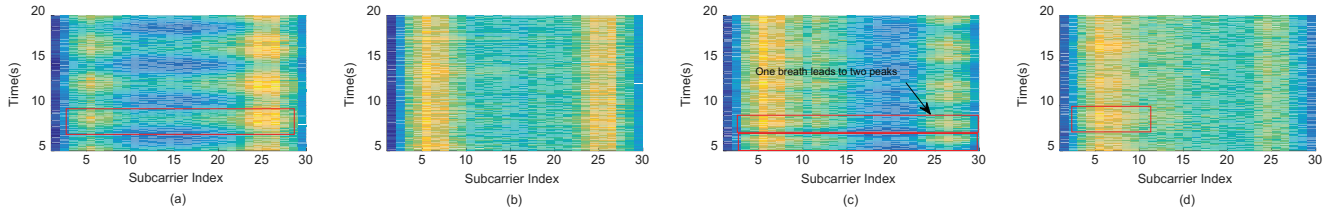

Figure 12. Evaluation of CSI subcarriers.

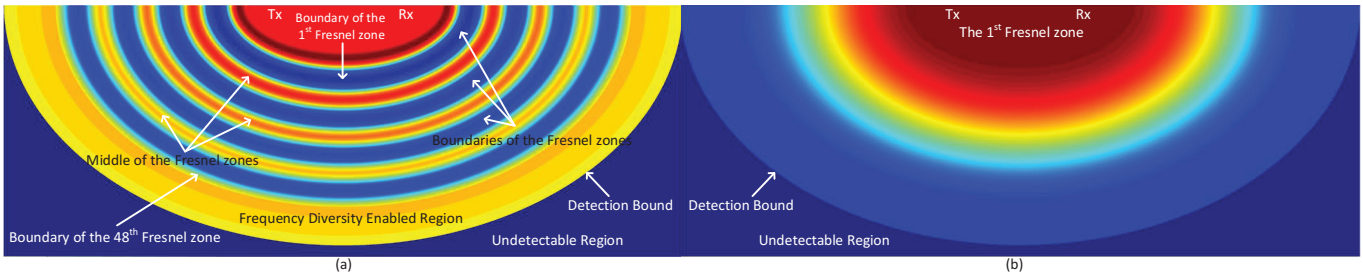

Figure 13. (a) User location heat map and (b) user orientation heat map (better viewed in color).

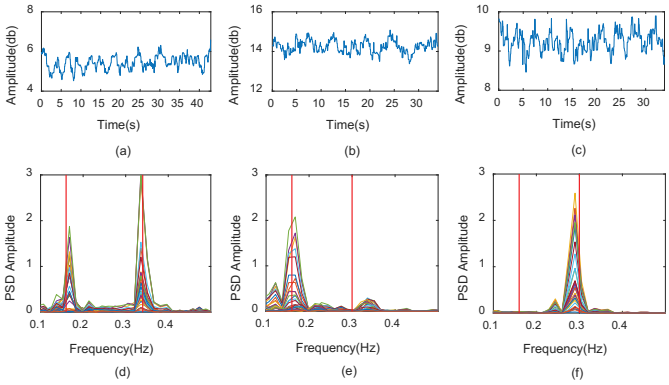

Figure 14. Two-person respiration detection: the red line indicates the ground truth; (a-c) time domain; (d-f) frequency domain.

the closer a subject is to the LOS, the clearer periodic patterns we obtain. In this experiment setting, the result shows that we are not able to detect respiration when a subject is $2m$ beyond the LOS along its perpendicular bisector (i.e., approximately the 110th Fresnel zone).

(2) Does Subject's Body Orientation Matter? We now study subject's body orientation, and evaluate how the system performs with respect to different body orientations in various locations of a Fresnel zone. Taking an example for illustration, a subject sits in the middle of the 2nd Fresnel zone, and changes his body orientation from 0°to 135°. The result is shown in Fig. 10 (c). From the figure, we observe that the most clear periodic pattern presents at 0°, and it starts fading when body orientation increases. After 90°, it becomes quickly flattening as the chest reflection surface is blocked by human body. With a similar experiment setting as above, we now move to the further Fresnel zones (i.e., 2nd, 3rd, etc) by increasing the distance to LOS. While we observe a similar trend, the body orientation range which can be detected keeps decreasing when going further away, as illustrated in Fig. 11.

(3) Impact of CSI Subcarriers Finally, we evaluate the impact of CSI subcarriers. We first evaluate if CSI subcarriers respond differently in a detectable area (i.e., ideal case). A subject is asked to sit close to the LOS in the middle of the 2nd Fresnel zone, and we plot the magnitude of each subcarrier in Fig. 12 (a). The figure shows the periodic patterns caused by human respiration is clear, and all the subcarriers give similar responses. We then conduct similar studies in the boundary of a Fresnel zone (i.e., worst case). A subject is now moved to the boundary of the 2nd Fresnel zone. Figure 12 (b) shows that no clear periodic patterns can be observed for all the subcarriers. With the same experimental setting, the subject is asked to take a deep breath, and as shown in Fig. 12 (b), we observe two double peaks present in each respiration cycle for all the subcarriers which matches our theoretical analysis. Finally, we evaluate another worst case scenario which a subject sits further away from the LOS. A subject moves 1m away from the LOS along the perpendicular bisector. As shown in Fig. 12 (d), we are now able to obverse the difference among subcarriers. We can see that the first five subcarriers respond obviously than all the others. Recall that in Equations (1) and (4), if $L = 100cm$, the bound is around $100cm$, if the first subcarrier fails to respond, at least one subcarrier (with 29 intervals) can be used. This proves our previous analysis that when a subject is far away from the LOS, we can leverage different CSI subcarriers to provide better detection.

(4) Discussions We now summarize the results we obtain so far, and revisit the questions we ask in the beginning. We plot the user location heat map in Figure 13(a), which shows how CSI signals vary with respect to different user locations. Several observations can be drawn from this map. First, there exist clear Fresnel zones in the space. The closer a subject is to the Tx/Rx, the stronger CSI signals we obtain. When a subject goes beyond a limit (i.e., detection bound), there are no clear CSI signals present to effectively detect human respiration. Second, in the region which is close to the de-

tection bound, which we name Frequency Diversity Enabled Region, there is no guarantee to successful detection unless we choose specific CSI subcarriers. Third, for each of the Fresnel zones, we observe strong CSI signals in the middle, but they start fading when moving towards the boundaries until no clear signals present at each boundary, resulting in detection failure. Figure 13(b) shows that how CSI signals vary with respect to different body orientations. Note that the figure is plotted when a subject is located in a detectable area (e.g., the middle of each Fresnel zone). We obverse that while we are able to detect a subject's body orientation from 0-90 degree in the Fresnel zones which are close to the Tx/Rx, body orientation we can detect keeps decreasing until 0 degree in the Fresnel zone which is close to the detection bound. Please note that while we achieve good results in the 1st Fresnel zone, the theoretic model in the cases which a subject blocks the LOS involves more complicated factors such as shadowing, diffusion, etc., which are subject to further study.

In summary, we conclude that user location and body orientation do influence the quality of CSI signals, and hence affect system performance when detecting human respiration. Through this case study, we verify the existence of the WiFi Fresnel zone and prove its properties in a real world setting, revealing the insights and new principles important for designing any CSI-based human respiration detection system.

B. Varying LOS Distance

In this experiment, we vary LOS distance to 0.5m, 2m, 3m, and 6m, respectively, and repeat the same experiments we did with fixed LOS distance. To ensure the first 12 Fresnel zones clear from reflectors such as the ground, the antenna heights are set to 50cm, 70cm, 70cm and 100cm with respect to the above LOS distance settings. We conduct the experiments for the first two cases (i.e., LOS = 0.5m, 2m) in the same office, but move to a large hall for the other two cases (i.e., LOS = 3m, 6m). We observe similar results as in our previous experiments. However, when the LOS distance is larger than 3m, the CSI signals become vulnerable with the environment noise, and it does not guarantee to be detected effectively even with the best user location and body orientation.

Case 2: Two Users with a Pair of WiFi Tx/Rx

Finally, we briefly present the multi-user case, using a two-user case as an example. A pair of WiFi Tx/Rx with 2m apart is deployed in a room. From the nine participants, we select six pairs who have different respiration rates and ask them to lie on a bed side-by-side between the Tx and Rx, as shown in Fig. 9. We first fix the Tx, then we intend to sense one person's breathing rate (without sensing the other's) and two subjects' breathing rates by changing the position of Rx. Figure 14 shows the results from three different scenarios. The upper figures in Fig. 14 are plotted in terms of the time domain while the lower figures are plotted in the frequence domain. Figures 14 (a,d) illustrates the first scenario where we successfully detect the respiratory rates for both subjects. In the second scenario (as shown in Figures 14 (b,e)), we purposely detect the respiratory rate of one subject but miss the other's, and vice versa in the third scenario in Figures 14 (c,f).

LIMITATIONS

The system has the following limitations: (1) for single-user respiration sensing, when some users are moving around in the proximity, the system might fail to detect one's respiration rate. However, when those users perform normal activities far from the subject and LOS, the subject's respiration rate could still be detected. (2) for the two-user case, the participants are assumed to have different breathing patterns so as to distinguish their breathing rates in the frequency domain. However, it is difficult to know whose breathing is whom's unless we assume different people have different and relative stable respiration patterns.

CONCLUSION AND FUTURE WORK

Starting from the recent work on WiFi CSI-based human respiration detection and other fine-grained human activity recognition, in our research we intend to ask and answer the questions like: Is it always possible to sense human respiration with a pair of WiFi devices no matter where a subject stays and faces in a room? What affects human respiration sensing and what's the theory behind in order to guide the respiration sensing system design? What is the possible physical limit for WiFi RF-based contactless sensing? Driven by the above questions, in this paper, we introduce a novel WiFi Fresnel model and develop the related theory to underpin the theoretical foundation for WiFi radio propagation in indoor environment. We apply our theory to the contactless human respiration detection application, and conduct comprehensive theoretical and experimental studies to investigate how user location, body orientation, and frequency diversity affect the respiration sensing performance. The obtained results not only prove the theory we developed, but also provide basic principles and practical guidelines for building cost-effective WiFi CSI-based human respiration sensing systems.

It is worth noting that while in this paper we apply our theory only in detecting human respiration, the theory can actually be applied to any RF-based sensing and detecting system in general. Further more, the work also sheds lights on understanding the physical limit of RF-based movement detection with numerous potential applications such as gesture recognition, virtual keyboard, etc. For our future work, on one hand, we plan to leverage higher transmission power, frequency diversity and multiple antennas to further improve the WiFi CSI-based respiration monitoring system; on the other hand, we intend to further develop the theory to understand issues such as how diffusion, reflection and shadowing interfere with each other and apply the developed theory to new applications.

ACKNOWLEDGMENT

This research is supported by National Key Research and Development Plan Grant No. 2016YFB1001200, NSFC Grant No. 61572048, the Capability Promotion Project of Shanghai State-owned assets supervision and Administration Commission under Grant No. 2014-C-1-02, Peking University Key Discipline Construction Grant. We wish to thank the anonymous reviewers for their excellent suggestions.

REFERENCES

1. Heba Abdelnasser, Khaled A Harras, and Moustafa Youssef. 2015. Ubibreathe: A ubiquitous non-invasive wifi-based breathing estimator. *arXiv preprint arXiv:1505.02388* (2015).
2. Gregory D Abowd, Aaron F Bobick, Irfan A Essa, Elizabeth D Mynatt, and Wendy A Rogers. 2002. The aware home: A living laboratory for technologies for successful aging. In *Proceedings of the AAAI-02 Workshop Automation as Caregiver*. 1–7.
3. Fadel Adib, Hongzi Mao, Zachary Kabelac, Dina Katabi, and Robert C Miller. 2015. Smart homes that monitor breathing and heart rate. In *Proceedings of the 33rd Annual ACM Conference on Human Factors in Computing Systems*. ACM, 837–846.
4. Gabriel Clavier Andre and Henri Darbord Rene. 1936. Directional radio transmission system. (June 9 1936). US Patent 2,043,347.
5. Robert E Collin. 1985. *Antennas and radiowave propagation*. McGraw-Hill.
6. Laurie Davies and Ursula Gather. 1993. The identification of multiple outliers. *J. Amer. Statist. Assoc.* 88, 423 (1993), 782–792.
7. H Erhan Dincer and William O'Neill. 2006. Deleterious effects of sleep-disordered breathing on the heart and vascular system. *Respiration* 73, 1 (2006), 124–130.
8. NHLBI: Health Information for the Public. U.S. Department of Health and Human Services. 2010. Sleep apnea: What is sleep apnea? (2010).
9. GigaOm. 2016. Could a breath-monitoring headset improve your health? `https://gigaom.com/2013/09/20/could-a-breath-monitoring-headset-improve-your-health/`. (2016). [Online; accessed 8-mar-2016].
10. Hulya Gokalp and Malcolm Clarke. 2013. Monitoring activities of daily living of the elderly and the potential for its use in telecare and telehealth: a review. *TELEMEDICINE and e-HEALTH* 19, 12 (2013), 910–923.
11. Daniel Halperin, Wenjun Hu, Anmol Sheth, and David Wetherall. 2011. Tool release: Gathering 802.11 n traces with channel state information. *ACM SIGCOMM Computer Communication Review* 41, 1 (2011), 53–53.
12. Chunmei Han, Kaishun Wu, Yuxi Wang, and Lionel M Ni. 2014. WiFall: Device-free fall detection by wireless networks. In *INFOCOM, 2014 Proceedings IEEE*. IEEE, 271–279.
13. Healthcare. 2012. F. M. Market for embedded health monitoring-gadgets to hit 170M devices by 2017. `http://www.fiercemobilehealthcare.com/story/market-embedded-health-monitoring-gadgets-hit-170m\-devices-2017/2012-08-03`. (2012).
14. Sumi Helal, William Mann, Jeffrey King, Youssef Kaddoura, Erwin Jansen, and others. 2005. The gator tech smart house: A programmable pervasive space. *Computer* 38, 3 (2005), 50–60.
15. Hristo D Hristov. 2000. *Fresnal Zones in Wireless Links, Zone Plate Lenses and Antennas*. Artech House, Inc.
16. Francis A Jenkins and Harvey E White. 1957. *Fundamentals of optics*. Tata McGraw-Hill Education.
17. Ossi Kaltiokallio, Huseyin Yigitler, Riku Jantti, and Neal Patwari. 2014. Non-invasive respiration rate monitoring using a single COTS TX-RX pair. In *Information Processing in Sensor Networks, IPSN-14 Proceedings of the 13th International Symposium on*. IEEE, 59–69.
18. T Kondo, T Uhlig, P Pemberton, and PD Sly. 1997. Laser monitoring of chest wall displacement. *European Respiratory Journal* 10, 8 (1997), 1865–1869.
19. James C Lin, Joseph Kiernicki, Martin Kiernicki, and Paul B Wollschlaeger. 1979. Microwave apexcardiography. *Microwave Theory and Techniques, IEEE Transactions on* 27, 6 (1979), 618–620.
20. Chen Liu, Dingyi Fang, Zhe Yang, Hongbo Jiang, Xiaojiang Chen, Wei Wang, Tianzhang Xing, and Lin Cai. 2016b. RSS Distribution-Based Passive Localization and Its Application in Sensor Networks. *IEEE Transactions on Wireless Communications* 15, 4 (2016), 2883–2895.
21. Jian Liu, Yan Wang, Yingying Chen, Jie Yang, Xu Chen, and Jerry Cheng. 2015. Tracking Vital Signs During Sleep Leveraging Off-the-shelf WiFi. In *Proceedings of the 16th ACM International Symposium on Mobile Ad Hoc Networking and Computing*. ACM, 267–276.
22. Xuefeng Liu, Jiannong Cao, Shaojie Tang, and Jiaqi Wen. 2014. Wi-Sleep: Contactless sleep monitoring via WiFi signals. In *Real-Time Systems Symposium (RTSS), 2014 IEEE*. IEEE, 346–355.
23. Xuefeng Liu, Jiannong Cao, Shaojie Tang, Jiaqi Wen, and Peng Guo. 2016a. Contactless Respiration Monitoring via WiFi Signals. *Mobile Computing, IEEE Transactions on* (2016).
24. C Lowanichkiattikul, M Dhanachai, C Sitathanee, S Khachonkham, and P Khaothong. 2016. Impact of chest wall motion caused by respiration in adjuvant radiotherapy for postoperative breast cancer patients. *SpringerPlus* 5, 1 (2016), 1–8.
25. Se Dong Min, Jin Kwon Kim, Hang Sik Shin, Yong Hyeon Yun, Chung Keun Lee, and Myoungho Lee. 2010. Noncontact respiration rate measurement system using an ultrasonic proximity sensor. *Sensors Journal, IEEE* 10, 11 (2010), 1732–1739.
26. M Nowogrodzki, DD Mawhinney, and HF Milgazo. 1984. Non-invasive microwave instruments for the measurement of respiration and heart rates. *NAECON 1984* (1984), 958–960.
27. Shoko Nukaya, Toshihiro Shino, Yosuke Kurihara, Kajiro Watanabe, and Hiroshi Tanaka. 2012. Noninvasive bed sensing of human biosignals via piezoceramic devices sandwiched between the floor and bed. *Sensors Journal, IEEE* 12, 3 (2012), 431–438.

28. Rita Paradiso. 2003. Wearable health care system for vital signs monitoring. In *Information Technology Applications in Biomedicine, 2003. 4th International IEEE EMBS Special Topic Conference on*. IEEE, 283–286.
29. Neal Patwari, Lara Brewer, Quinn Tate, Ossi Kaltiokallio, and Maurizio Bocca. 2014a. Breathfinding: A wireless network that monitors and locates breathing in a home. *Selected Topics in Signal Processing, IEEE Journal of* 8, 1 (2014), 30–42.
30. Neal Patwari, James Wilson, Sundaram Ananthanarayanan, Sneha Kumar Kasera, and Dwayne R Westenskow. 2014b. Monitoring breathing via signal strength in wireless networks. *Mobile Computing, IEEE Transactions on* 13, 8 (2014), 1774–1786.
31. Anders N Pedersen, Stine Korreman, Håkan Nyström, and Lena Specht. 2004. Breathing adapted radiotherapy of breast cancer: reduction of cardiac and pulmonary doses using voluntary inspiration breath-hold. *Radiotherapy and oncology* 72, 1 (2004), 53–60.
32. Jochen Penne, Christian Schaller, Joachim Hornegger, and Torsten Kuwert. 2008. Robust real-time 3D respiratory motion detection using time-of-flight cameras. *International Journal of Computer Assisted Radiology and Surgery* 3, 5 (2008), 427–431.
33. Ruth Ravichandran, Elliot Saba, Ke-Yu Chen, Mayank Goel, Sidhant Gupta, and Shwetak N Patel. 2015. WiBreathe: Estimating respiration rate using wireless signals in natural settings in the home. In *Pervasive Computing and Communications (PerCom), 2015 IEEE International Conference on*. IEEE, 131–139.
34. Stefano Savazzi, Stephan Sigg, Monica Nicoli, Vittorio Rampa, Sanaz Kianoush, and Umberto Spagnolini. 2016. Device-Free Radio Vision for Assisted Living: Leveraging wireless channel quality information for human sensing. *IEEE Signal Processing Magazine* 33, 2 (2016), 45–58.
35. David Tse and Pramod Viswanath. 2005. *Fundamentals of wireless communication*. Cambridge university press.
36. Svetha Venkatesh, Christopher R Anderson, Natalia V Rivera, and R Michael Buehrer. 2005. Implementation and analysis of respiration-rate estimation using impulse-based UWB. In *Military Communications Conference, 2005. MILCOM 2005. IEEE*. IEEE, 3314–3320.
37. Pierre-Frédéric Villard, Piers Boshier, Fernando Bello, and Derek Gould. 2011. *Virtual reality simulation of liver biopsy with a respiratory component*. InTech.
38. Hao Wang, Daqing Zhang, Yasha Wang, Junyi Ma, Yuxiang Wang, and Shengjie Li. 2016. RT-Fall: A Real-time and Contactless Fall Detection System with Commodity WiFi Devices. *Mobile Computing, IEEE Transactions on* (2016).
39. Wei Wang, Alex X Liu, Muhammad Shahzad, Kang Ling, and Sanglu Lu. 2015. Understanding and modeling of wifi signal based human activity recognition. In *Proceedings of the 21st Annual International Conference on Mobile Computing and Networking*. ACM, 65–76.
40. Joey Wilson and Neal Patwari. 2011. See-through walls: Motion tracking using variance-based radio tomography networks. *Mobile Computing, IEEE Transactions on* 10, 5 (2011), 612–621.
41. James C Wiltse. 1999. History and evolution of Fresnel zone plate antennas for microwaves and millimeter waves. In *Antennas and Propagation Society International Symposium, 1999. IEEE*, Vol. 2. IEEE, 722–725.
42. Chenshu Wu, Zheng Yang, Zimu Zhou, Xuefeng Liu, Yunhao Liu, and Jiannong Cao. 2015. Non-Invasive Detection of Moving and Stationary Human With WiFi. *Selected Areas in Communications, IEEE Journal on* 33, 11 (2015), 2329–2342.
43. Daqing Zhang, Hao Wang, Yasha Wang, and Junyi Ma. 2015. Anti-fall: A Non-intrusive and Real-Time Fall Detector Leveraging CSI from Commodity WiFi Devices. In *Inclusive Smart Cities and e-Health*. Springer, 181–193.